



Energy equilibrium of cleavage front transmission across a high-angle grain boundary in a free-standing silicon thin film

Yu Qiao ^{a,*}, Jin Chen ^a, Xinguo Kong ^b, Srinivas S. Chakravarthula ^b

^a Department of Structural Engineering, University of California – San Diego, La Jolla, CA 92093-0085, USA

^b Department of Civil Engineering, University of Akron, Akron, OH 44325-3905, USA

Received 18 October 2005; received in revised form 2 August 2007; accepted 2 August 2007

Available online 11 August 2007

Abstract

In this article, the crack growth driving force and the resistance to cleavage cracking associated with crack front transmission across a high-angle grain boundary in a silicon thin film are analyzed, and a closed-form solution of grain boundary toughness is obtained. It is noticed that the fracture resistance of the grain boundary is a function of the film thickness. This size effect is attributed to the nonuniform nature of cleavage front advance.

© 2007 Elsevier Ltd. All rights reserved.

Keywords: Thin film; Toughness; Grain boundary; Size effect

1. Introduction

One of the intrinsic difficulties in assuring reliable service of thin film materials is that most of them are brittle at working temperatures. Under unexpected external loadings or residual stresses, catastrophic failure can take place, often resulting in the failure of the entire device [1]. Over many decades, understanding their fracture resistances has been an active research area [2–4].

One of the most widely used thin film materials is silicon. Depending upon the deposition procedure and the thermal treatment history, the grain structure of a silicon thin film can be amorphous, columnar, or equiaxed [5]. Amorphous silicon films are usually formed when the substrate temperature is relatively low [6]. Due to the poor mechanical and electrical properties, they are seldom used in microfabrication. When the substrate temperature is relatively high, silicon crystallizes and, because the grain nuclei with unfavorable orientations would be buried, the grain structure is often through-thickness [7,8]. The grain boundaries, which would interrupt the cleavage cracking process from grain to grain, offer higher fracture resistance compared with single crystals, and thereby dominate the fracture behavior. For instance, grain-sized microcracks have been observed frequently in both scientific research and engineering practice [9,10], indicating clearly that, before

* Corresponding author. Tel.: +858 534 3388; fax: +858 822 2260.

E-mail address: yqiao@ucsd.edu (Y. Qiao).

a short crack can grow into a long one, it must overcome the grain boundaries in its propagation path. With the increasingly high functional requirements, the reliability analysis of silicon thin films becomes more and more critical in the design of microelectromechanical systems and electronics packaging.

While the cleavage cracking across grain boundaries is an important phenomenon, the systematic studies on it are scarce. Recently, Qiao and Argon [11] performed an experimental investigation on the grain boundary toughness of a substantial set of brittle iron–silicon bicrystals. It was observed that, as a cleavage front overcame a high-angle grain boundary, the grain boundary was not broken through uniformly. Rather, the cleavage front first penetrated across the grain boundary at a number of break-through points, leaving the persistent grain boundary islands (PGBI) behind. The role of PGBI was quite similar with that of hard reinforcements in a composite that toughen the material through both crack trapping and bridging. Eventually, as the penetration depth of the crack front across the grain boundary reached a critical value, the PGBI would be sheared apart. In this experiment, because the samples were much larger than the width of the break-through window, there were a large number of break-through points distributed along the grain boundary. Therefore, although the distance between the break-through points varied in a relatively large range from 1 to 10 μm , the effect of the variation was averaged out, leading to a size independent boundary toughness [12,13]. In a thin film material, on the other hand, if the grain boundary is relatively narrow such that only one or a limited number of break-through points can be developed, the front transmission across the grain boundary can be constrained by the film surfaces, which in turn affects the fracture resistance.

In order to analyze the fracture toughness of thin films, details of cleavage front advance must be taken into consideration. In a previous study [14], we analyzed the energy equilibrium of the cleavage cracking across an infinitely wide grain boundary. In the current research, we will examine the cleavage front transmission across a narrow through-thickness grain boundary.

2. Cleavage front transmission across a narrow grain boundary

When a cleavage front encounters a grain boundary, as previously discussed, the front transmission is dominated by the formation and growth of break-through points. The distance of the break-through points, according to the statistical analysis of experimental data [11], is a material constant independent of the crystallographic orientations. If the film thickness, t , is comparable with or even smaller than this characteristic length, the width of the grain boundary is large enough for only one break-through point, as shown in Fig. 1 and also depicted in Fig. 2a. The cleavage front would first penetrate across the grain boundary in the break-through window. The sections of the front near the film surfaces would be arrested by the persistent grain boundary areas.

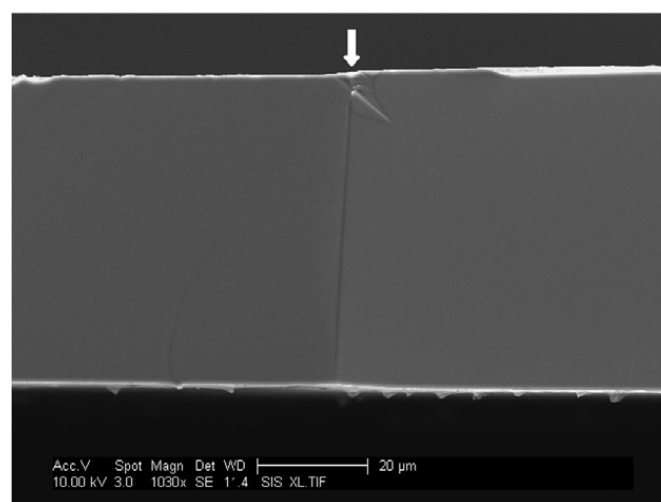


Fig. 1. SEM microscopy of cleavage cracking across a through-thickness grain boundary in a silicon thin film. The crack propagated from the right to the left. The arrow indicates the grain boundary.

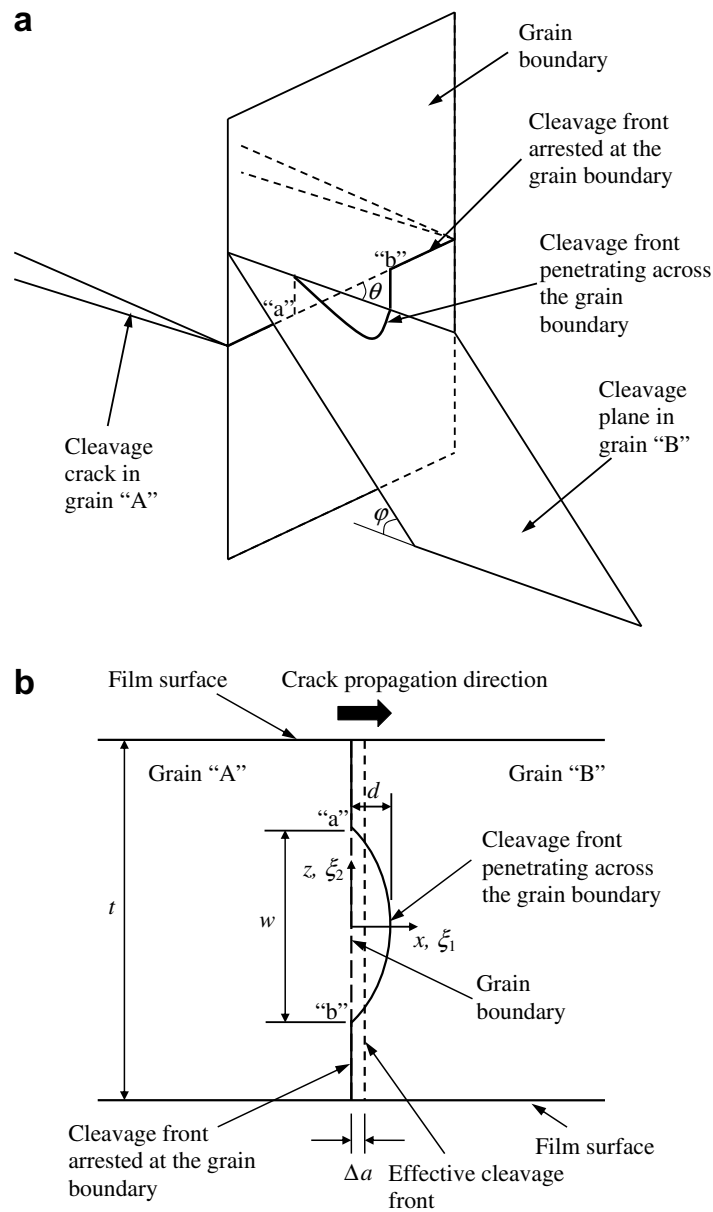


Fig. 2. Schematic of a cleavage front penetrating across a narrow grain boundary: (a) three dimensional view; and (b) top view. Section “ab” indicates the break-through window.

According to the profile of river markings, the contour of the cleavage front in the break-through window can be described by a power-law function [14]

$$\xi_2 = \pm(\tilde{d} - \xi_1)^\beta \quad (1)$$

where $\xi_1 = x/t$; $\xi_2 = z/t$, with z being the grain boundary direction; β is a parameter in the range of 0.5–0.7; and $\tilde{d} = (w/2t)^{1/\beta}$ is the normalized penetration depth at the crest of the verge of propagating, with w being the width of break-through window (see Fig. 2b). The fracture work associated with the crack front penetration can be stated as

$$W = W_B + W_{GB} \quad (2)$$

where W_B is the work of separation of the cleavage surface in grain “B” and W_{GB} is the work required to shear apart the grain boundary inside the break-through window. Note that W_B can be calculated as

$$W_B = G_B \cdot \left\{ 2t^2 \int_0^{w/2t} \left[\left(\frac{w}{2t} \right)^{\frac{1}{\beta}} - \zeta_2^{\frac{1}{\beta}} \right] d\zeta_2 \right\} = \frac{2G_B t^2}{1 + \beta} \left(\frac{w}{2t} \right)^{\frac{1+\beta}{\beta}} \quad (3)$$

where G_B is the fracture resistance of grain “B”. The integration term in Eq. (3) gives the area of the cleavage facet ahead of the grain boundary.

The work of separation of the grain boundary in the break-through window can be stated as

$$W_{GB} = (2\gamma_{GB})[(w/2)^2 \tan \theta] \quad (4)$$

where γ_{GB} is the effective surface free energy of grain boundary, and θ is the twist misorientation. The effective crack front can be taken as the line passing through the centroid of the penetration area. Hence, the effective crack growth distance is

$$\Delta a = \frac{2t}{1 + \beta} \left(\frac{w}{2t} \right)^{\frac{1+\beta}{\beta}} \quad (5)$$

Substitution of Eqs. (3)–(5) into (2) gives

$$W = G_B t(a - a_0) + (2\gamma_{GB}) \tan \theta \cdot t^2 \left[\frac{(a - a_0)(1 + \beta)}{2t} \right]^{\frac{2\beta}{1+\beta}} \quad (6)$$

The fracture resistance offered by the grain boundary can then be obtained as

$$R(a) = \frac{1}{t} \frac{\partial W}{\partial a} = G_B + \beta \cdot (2\gamma_{GB}) \tan \theta \cdot \left[\frac{\Delta a \cdot (1 + \beta)}{2t} \right]^{\frac{\beta-1}{\beta+1}} \quad (7)$$

Eq. (7) indicates that, with the increasing of the penetration depth, since more and more grain boundary area is separated, the fracture resistance of grain boundary, R , rises, and therefore the crack growth driving force, G , must be raised to drive the crack front deeper into grain “B”. The grain boundary induced position dependence of fracture resistance makes the transgranular cracking fundamentally different from the cracking in a single crystal.

For the sake of simplicity, we analyze the contoured thin film sample depicted in Fig. 3. It will be shown shortly that the sample geometry does not affect the calculation result of the fracture resistance of grain boundary, G_{cr} . The contour of the sample is $12x/y^3 + 3(1 + \nu)/(xy) = m$, where $\{x, y\}$ is the coordinate system, with x being the crack growth direction and y the normal of fracture surface; ν is the Poisson’s ratio; and m is the geometry factor. Based on a discussion of the constant- K specimen [15], the compliance of this specimen is

$$C = \frac{\delta}{P} = \frac{ma^2}{Et} \quad (8)$$

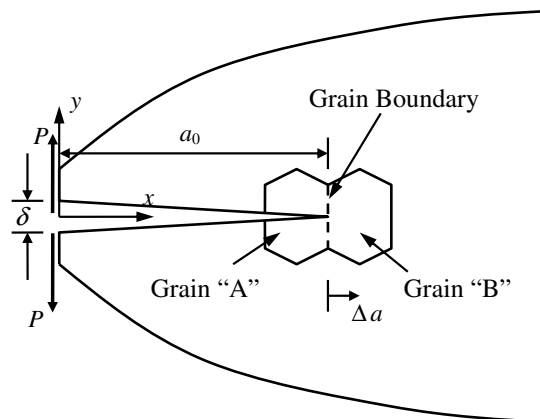


Fig. 3. The contoured thin film sample.

where P and δ are the crack opening load and displacement, respectively, E is the modulus of elasticity, t is the sample thickness, and a is the crack length. With a given load, P , the energy release rate is

$$G = \frac{P^2}{2t} \frac{\partial C}{\partial a} = \frac{ma}{E} \left(\frac{P}{t}\right)^2 \quad (9)$$

It can be seen that G is proportional to a ; that is, without changing the applied load, the crack growth driven force increases linearly as the crack advances.

In general case, in a material where the fracture resistance increases with the crack growth length, the crack growth stability can be well described in the framework of R -curve analysis e.g. [16], as shown in Fig. 4. In the bicrystal sample, due to the grain boundary separation, according to Eq. (7), the fracture resistance is a function of the effective crack length. Initially, when $P = P_1$ is relatively small, with the initial crack length of a_0 , the energy release rate is lower than the fracture resistance of grain “B”, G_B , and the crack does not propagate. According to Eq. (9), the crack growth starts at $G = G_B$, i.e. $P/t = \sqrt{EG_B/ma_0}$. Since $\partial G/\partial a$ is initially smaller than $\partial R/\partial a$, as the crack grows by a infinitesimal distance, G would be lower than R , and the crack would immediately stop, until the applied crack opening load is increased. That is, the crack growth is stable.

With the increasing of the penetration depth of the crack front across the grain boundary, the effective growth distance, Δa , keeps rising. While the fracture resistance, R , increases with a , the magnitude of $\partial R/\partial a$ is reduced. Eventually, when

$$\frac{\partial R}{\partial a} = \frac{\partial G}{\partial a} \quad (10)$$

further increase in a would result in unstable crack advance, causing the final failure of the grain boundary. Consequently, the grain boundary toughness, G_{cr} , should be taken as the point in the R -curve that satisfies Eq. (10), which, based on Eq. (9), can be rewritten as

$$\frac{\partial R}{\partial a} = \frac{R}{a} \quad (11)$$

Consequently, the normalized excess fracture resistance of grain boundary is

$$\tilde{G} = \frac{G_{cr}}{G_B} - 1 = \frac{\beta \cdot \tan \theta}{\tilde{G}_B} \left[\frac{\Delta a_{cr} \cdot (1 + \beta)}{2t} \right]^{\frac{\beta-1}{\beta+1}} \quad (12)$$

where Δa_{cr} is the critical penetration depth at the onset of the grain boundary failure and $\tilde{G}_B = G_B/2\gamma_{GB}$.

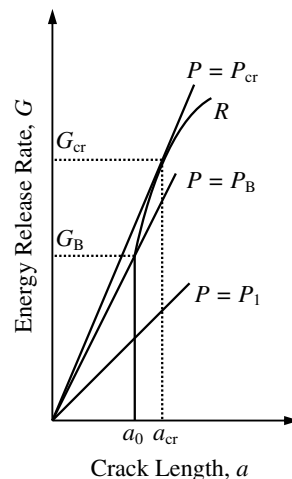


Fig. 4. The energy equilibrium at a cleavage front transmitting across a high-angle grain boundary.

Finally, combination of Eqs. (7), (9), and (12) leads to

$$\left[\frac{1-\beta}{2t} a_0 + \frac{1-\beta}{1+\beta} \left(\frac{\tilde{G}\tilde{G}_B}{\beta \cdot \tan \theta} \right)^{\frac{\beta+1}{\beta-1}} \right] \left(\frac{\tilde{G}\tilde{G}_B}{\beta \cdot \tan \theta} \right)^{\frac{2}{1-\beta}} = \frac{(1+\tilde{G})\tilde{G}_B}{\beta \cdot \tan \theta} \quad (13)$$

solving which gives \tilde{G} . In the above derivation, the variant of Eq. (12),

$$\Delta a_{cr} = \frac{2t}{1+\beta} \left[\frac{\tilde{G}\tilde{G}_B}{\beta \cdot \tan \theta} \right]^{\frac{\beta+1}{\beta-1}}$$

and the relationships of $a = a_0 + \Delta a_{cr}$ and $G = R$ are utilized.

3. Results and discussion

Although the above discussion is based on the analysis of the contoured sample shown in Fig. 3, the sample geometry does not affect the result of \tilde{G} as long as the G – a relationship is governed by Eq. (9), since the geometry factor, m , vanishes in Eq. (13). Under this condition, when m tends to infinity, the contoured sample converges to an infinitely large half plane.

For silicon, the effective surface free energy of grain boundary is about 80% of that of a single crystal, and G_B can be estimated as $2\gamma/\cos\theta\cos\varphi$ [11], where γ is the effective surface free energy of cleavage plane and φ is the tilt crystallographic misorientation. The results of Eq. (13) are shown in Fig. 5, with both of θ and φ being set to 20° . It can be seen that, due to the grain boundary effect, there is an about 5–15% increase in fracture resistance, depending on the film thickness and the contour of penetrating crack front. As the film thickness increases, since more grain boundary would be involved in the front transmission, both of R and $\partial R/\partial a$ vary, and thereby the critical condition of Eq. (10) is more difficult to reach, leading to a higher G_{cr} . This size effect is more pronounced when the film thickness is smaller. As the film thickness approaches the level of the crack length, the grain boundary toughness becomes quite insensitive to it. Note that, when t is large, there can be more than one break-through points along the boundary, and thus the size effect would be “saturated” and this model is no longer valid.

Through Fig. 5, it is clear that \tilde{G} is also affected by the crack length, a_0 ; that is, G_{cr} is not a material constant. The fracture resistance of a grain boundary is smaller for a longer crack. Without considering other factors, as a_0 tends to infinity, the excess fracture resistance caused by the grain boundary converges to 0, and thus $G_{cr} \rightarrow G_B$. The crack length dependence is a typical result of the R -curve analysis, which reflects the complexity of the fracture behavior of heterogeneous materials. At the tip of a longer crack, the grain boundary

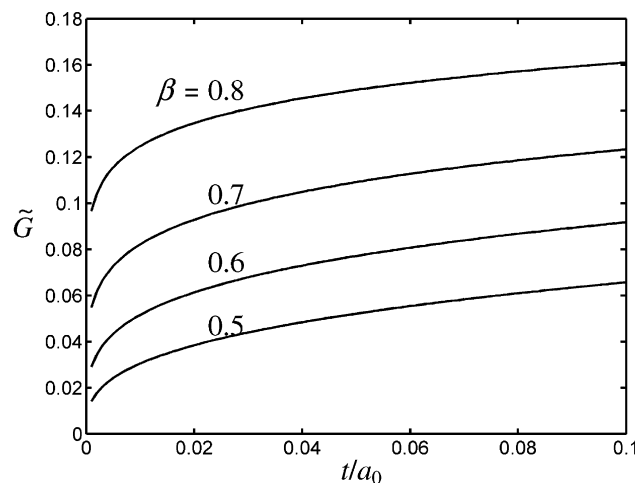


Fig. 5. The excess grain boundary resistance as a function of the film thickness.

width looks “smaller”, and eventually when $a_0 \gg t$ only the crack length independent part of the fracture resistance caused by the crystallographic misorientations remains.

The factor of the contour of the penetrating crack front, which is characterized by β , comes in by affecting the increasing rate of the R -curve and the effective crack growth distance. The larger the value of β , the “sharper” the penetrating cleavage front is. Note that when $\beta = 0.5$ the penetrating crack front is a part of a circle and when $\beta = 1$ the front consists of straight lines. As β increases, with the same width of break-through window, w , more cleavage facet would be produced in grain “B” before the grain boundary finally fails. On the other hand, less grain boundary area would be involved in the front transmission, which tends to lower the grain boundary toughness. Fig. 5 indicates that the former mechanism is more important. The value of β can be estimated based on the contour of river markings, which has been determined to be about 0.6 in a previous analysis for an iron–silicon alloy [14]. In the current study, β is taken as a material constant in the range of 0.4–0.8. As β increases from 0.5 to 0.8, G_{cr} increases by a factor of about 2. The details of the front penetration are still under investigation. It is likely that β is dominated by the stress field, loading rate, as well as the local microstructure.

Fig. 6 shows the normalized grain boundary resistance, $\tilde{G}_{cr} = G_{cr}/(2\gamma)$, as a function of the crystallographic misorientations, where β and t/a_0 are set to 0.7 and 0.05, respectively. The value of \tilde{G}_{cr} increases with both the twist and the tilt angles, while the influence of the former is more significant. This result is consistent with the experimental observation of the cleavage cracking across a field of randomly misorientated grains [12].

For a number of engineering applications, an approximate regression equation can be useful for a quick assessment of fracture resistance. According to Eq. (13), with a given β , the grain boundary toughness is a function of $\{\hat{G}, \tilde{t}\}$, where $\hat{G} = \tilde{G}_B/\beta \tan \theta$ and $\tilde{t} = t/a_0$. Since as \hat{G} tends to 0, $\tilde{G} \rightarrow \infty$; and as \tilde{t} is infinitesimal, $\tilde{G} \rightarrow 0$, the numerical results may be expressed as a two-power-law equation

$$\tilde{G} = \zeta_1 \hat{G}^{\zeta_2} \tilde{t}^{\zeta_3} \tag{14}$$

where ζ_i ($i = 1, 2, 3$) are parameters obtained by the least mean square method, and their values are given in Table 1. Note that ζ_2 must be negative. The factor of \hat{G} collectively captures the material properties and the microstructures, such as the crystallographic orientations, fracture resistance of crystal plane, as well as the geometry of the crack front. The factor of \tilde{t} reflects the size effect, including the influences of the film thickness and the crack length.

It is clear that the above discussion gives only a first-order estimation of the grain boundary toughness. A number of details associated with the crack front transmission, for instance the effect of anisotropy, the nature of grain boundary shearing, and the competition between crack front penetration and break-through window expansion, are not taken into account. The critical condition is taken as the onset of the unstable crack growth. Any post-critical dynamic effect is beyond the scope of the current study. Furthermore, the assumption that the material is purely brittle makes this model irrelevant to ductile materials. Nevertheless, this investigation predicts the size dependence of the fracture resistance of polycrystalline thin films, which provides a basis for the experimental study. Note that in the above discussion, it is assumed that the grain boundary is

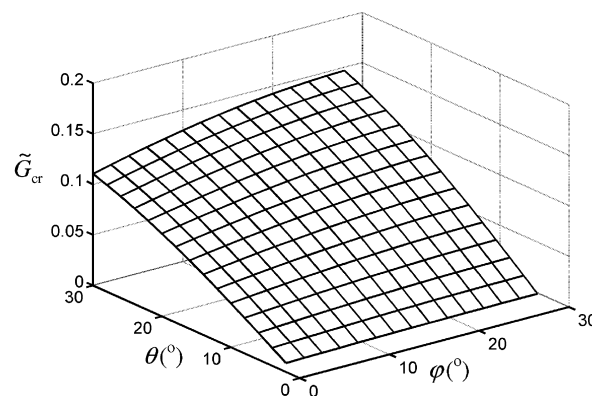


Fig. 6. The excess grain boundary resistance as a function of the crystallographic misorientations.

Table 1
The parameters of the regression equation

β	ζ_1	ζ_2	ζ_3
0.4	18.8	−1.10	0.64
0.5	15.0	−0.98	0.61
0.6	14.4	−0.85	0.52
0.7	11.6	−0.79	0.46
0.8	11.1	−0.75	0.42

separated apart simultaneously as the cleavage front bypasses it. The associated increase in fracture resistance is about 5–15% of crystallographic resistance, which is relatively small compared with experimental observations [17,18]. Since the crack trapping effect of the grain boundary is ignored, the result of G_{cr} should be regarded as a lower estimate. If the grain boundary is assumed tough, i.e. the persistent grain boundary areas do not fail even after the crack front transmits into grain “B”, the crack trapping effect can offer a much higher resistance increase around 100% [19], which should be taken as an upper estimate. The actual grain boundary toughness is likely in between of them.

4. Conclusions

The fracture resistance of a through-thickness grain boundary to cleavage cracking in a silicon thin film is investigated in context of R -curve analysis. The cleavage front first penetrates across the grain boundary in a break-through window. The grain boundary fails as the critical penetration depth is reached such that the increasing rate of fracture resistance is lower than that of the crack growth driving force. This model gives a lower estimate of the grain boundary toughness. The following conclusions are drawn:

1. For microcracks shorter than 500 times of the film thickness, the excess fracture resistance of grain boundary must be taken into consideration.
2. Due to the nonuniform nature of the cleavage front transmission across grain boundary, the grain boundary resistance is increased by about 5–15% compared with that of single crystal.
3. The fracture resistance of grain boundary increases with film thickness.

Acknowledgement

This work was supported by the US Department of Energy, Office of Basic Energy Sciences under Contract DE-FG02-07ER46355.

References

- [1] Ohring M. Materials science of thin films. NY: Academic Press; 1991.
- [2] Madou MJ. Fundamentals of microfabrication. NY: CRC Press; 2002.
- [3] Hutchinson JW, Evans AG. Acta Mater 2000;48:125.
- [4] Gao H, Huang Y, Nix WD, Hutchinson JW. J Mech Phys Solids 1999;47:1239.
- [5] Senturia SD. Microsystem design. Boston, MA: Kluwer; 2000.
- [6] Thompson CV. Annu Rev Mater Sci 2000;30:159.
- [7] Srolovits DZ. J Vac Sci Technol A 1986;4:2925.
- [8] Joubert P, Sarret M, Haji L, Hamedi L, Loisel B. J Appl Phys 1989;66:4806.
- [9] Sharpe WN, Yuan B, Edwards RL. J Micromech Microeng 1997;6:193.
- [10] Greek S, Ericson F, Hohansson S, Furttsch M, Rump A. J Micromech Microeng 1999;9:245.
- [11] Qiao Y, Argon AS. Mech Mater 2003;35:313.
- [12] Qiao Y, Argon AS. Mech Mater 2003;35:129.
- [13] Qiao Y, Kong X. Mater Lett 2004;58:3156.
- [14] Qiao Y. Mater Sci Eng A 2003;361:350.
- [15] Mostovoy S, Crosley PB, Ripling EJ. J Mater 1967;2:661.

- [16] Hertzberg RW. Deformation and fracture mechanics of engineering materials. New York: John Wiley & Sons; 1989.
- [17] Chasiotis I, Cho SW, Jonnalagadda KJ. Appl Mech – Trans ASME 2006;73:714.
- [18] McCarty A, Chasiotis I. Thin Solid Films 2007;515:3267.
- [19] Qiao Y, Kong X. Mech Mater 2007;39:746.